Available online at www.sciencedirect.com

ScienceDirect

Scripta Materialia 86 (2014) 24–27

Scripta MATERIALIA

www.elsevier.com/locate/scriptamat

Multiple and extended shear band formation in MgCuGd metallic glass during high-pressure torsion

Baolong Zheng,[a] Yizhang Zhou,[a] Suveen N. Mathaudhu,[b] Ruslan Z. Valiev,[c] Chi Y.A. Tsao,[d] Julie M. Schoenung[a] and Enrique J. Lavernia[a,*]

[a] *University of California—Davis, Davis, CA 95616, USA*
[b] *US Army Research Laboratory, Aberdeen Proving Ground, MD 21005, USA*
[c] *Ufa State Aviation Technical University, Ufa 450000, Russia*
[d] *National Cheng Kung University, Tainan 701, Taiwan, ROC*

Received 2 January 2014; revised 24 April 2014; accepted 24 April 2014
Available online 2 May 2014

$Mg_{65}Cu_{25}Gd_{10}$ bulk metallic glass (BMG), containing a high density of intersecting extended shear bands (SBs), was fabricated from densification of amorphous powder via high-pressure torsion (HPT). The extended SBs, up to 400 nm in width and containing nanocrystalline structures, were studied by electron microscopy. The mechanisms responsible for the formation of the high density of extended SBs are discussed and related to the high hydrostatic pressure and shear strains imposed during HPT of BMGs.

Keywords: Metallic glass; High-pressure torsion; Shear bands; Powder

Glass-forming alloys are frequently synthesized as powders or ribbons, because with these geometries it is relatively trivial to achieve the high cooling rates (e.g. 10^3–10^5 K s^{-1}) that are required to avoid crystallization [1,2]. Accordingly, gas atomization has been successfully used for the fabrication of metallic amorphous powders, which can be subsequently consolidated into bulk metallic glasses (BMGs) using well-established thermomechanical methods [3–5].

More recently, the severe plastic deformation technique of high-pressure torsion (HPT) has been used to consolidate powders and study their response to high strain levels [3,4]. HPT introduces large amounts of plastic deformation via rotation of a disc-shaped specimen under high pressures ($P > 4$ GPa). The characteristics of HPT processing include high hydrostatic pressure and large superimposed shear strains ($\gamma > 1000$, equivalent to a true strain ε of 6.9) with a limited temperature increase (<283 K) [3,5].

Inspection of the literature reveals few studies describing HPT of BMGs, partly due to the poor formability and plasticity of BMGs at room temperature. Unlike crystalline metals, deformation via dislocation and twinning mechanisms is not possible in the case of BMGs. BMGs deform in a highly localized mode, where a large amount of plastic strain is accumulated in very thin (~10–100 nm) narrow regions, known as shear bands (SBs). SBs exhibit strain-softening behavior [6], and are important in BMGs because the associated strain-softening leads to plastic instability during deformation [7]. It has been reported that the formation of multiple SBs throughout BMGs can enhance its plasticity via the introduction of "plastically soft" regions. Because each band contributes to the overall plasticity and none carry sufficient deformation to cause catastrophic failure, room-temperature formability can be enhanced [8].

In this research we report, for the first time, the synthesis of BMGs by consolidation of amorphous powder using HPT, paying particular attention to mechanisms governing the in situ formation of high-density extended SBs with nanocrystalline (nc) grains. The objective of our study is to provide preliminary insight into the mechanisms that govern the initiation, activation and behavior of SBs formed during HPT, using scanning electron microscopy (SEM), transmission electron microscopy (TEM) and differential scanning calorimetry (DSC) results as the basis.

* Corresponding author. Tel.: +1 530 752 9568; fax: +1 530 752 9554; e-mail: bzheng@ucdavis.edu

http://dx.doi.org/10.1016/j.scriptamat.2014.04.023
1359-6462/

In our experiments, gas-atomized $Mg_{65}Cu_{25}Gd_{10}$ amorphous powder, with an approximate size of 150 μm, was HPTed under a pressure of 6 GPa and five turns at room temperature. The turning speed was 0.2 rpm. BMG discs approximately 10 mm in diameter and 1 mm in thickness were prepared.

TEM studies were conducted on thin foils of HPTed MgCuGd BMGs that were prepared via mechanical grinding and polishing to a thickness of ~30 μm, followed by ion milling (Gatan PIPS-691) to a thickness suitable for electron transparency. A Philips CM-12 microscope was used for TEM micrograph and selected-area electron diffraction (SAED) analysis.

Figure 1 shows an SEM micrograph of an MgCuGd BMG disc consolidated via HPT of gas-atomized amorphous powder. The SEM images were taken from positions near the upper surface and near the center of the HPTed BMG radius. The absence of cracks and interfaces between particles was evident on the surface of the HPTed BMG discs. In general, it is difficult to achieve complete interparticle metallurgical bonding between the metallic glass powders due to the presence of a surface oxide film, which acts as a diffusion barrier and limits the mass transfer required for complete densification [9,10]. In the case of HPT, the action of intense shear strains (~150) and normal compressive stresses (6 GPa) effectively disrupt surface oxides, thereby facilitating metal-to-metal contact, and enhancing the kinetics of interface metallurgical bonding formation between particles [11,12].

The formation and evolution of SBs represents the only bulk plasticity mechanism during the deformation of MgCuGd amorphous powder at temperatures far lower than T_g (420 K) [3]. Figure 1 shows that there is a high density of SBs on the surface of HPTed MgCuGd BMGs. Moreover, multiple SBs can be discerned as vein patterns with different orientations. It was also observed that there are some primary SBs, with a width >100 nm, and a large number of secondary SBs with a width <100 nm, as highlighted by arrows in Figure 1. The secondary SBs appeared to have originated at primary SBs, and evolved with different orientations. The patterns of primary and secondary SBs exhibit spacings of 1–2 and 0.2–0.6 μm, respectively. Interestingly, the density of SBs in our study is over three orders of magnitude higher than that in a PtCuNiP BMG deformed in tension; in that study the spacing of the primary and secondary SBs was 5–10 and 0.3–0.9 mm, respectively [13]. The presence of a high density of SBs can be rationalized on the basis of the imposition of high shear strains in combination with high hydrostatic compression stress during HPT [5], which can suppress SB separation, and thereby avoid premature crack nucleation as in the case of tension. During tensile deformation, the detachment stress on the SBs can enhance strain softening and promote instability, resulting in the nucleation of a few cracks that propagate rapidly [6,7]. Hence the presence of high hydrostatic compressive stress during HPT effectively promotes the formation of multiple SBs, which can better accommodate deformation.

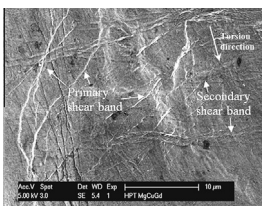

Figure 1. SEM micrograph showing the high density of SBs in HPTed $Mg_{65}Cu_{25}Gd_{10}$ BMG.

The origin of the observed network of SBs can be explained on the basis of interactions between the SBs, which increase the local stress field and nucleate SB branches to release localized stress concentration and accommodate surrounding shear strains. During HPT, SBs that are initiated in high-stress or plastically soft regions are arrested in surrounding regions having higher yield stress or stiffness, or at intersecting SBs. This inhomogeneous mode of deformation occurs under conditions of high applied stresses and temperatures $< T_g$. In the presence of high hydrostatic compressive stress, the primary SBs can grow continuously and carry the plastic strain without nucleating cracks. Moreover, some small, wing-like branch bands were found along primary SBs, suggesting that the SB branches can grow and interact, leading to the formation of a network that can sustain the overall strain during deformation. The primary SBs appear wavy, and the periodicity of the wave is ~0.2–0.6 μm, which is consistent with the observed interspace between secondary SBs. BMGs deformed by HPT reveal a high density of SBs which form polycrystal-like patterns that effectively behave as "grain boundaries", leading to a deformation mode that is analogous to grain boundary gliding in nanostructured materials [8]. It was reported that the room-temperature formability of BMGs can be enhanced by introducing "plastically soft" regions. Hence, even though the plastic strain is localized in the SBs, the BMGs appear to deform in a macroscopically near-homogeneous manner due to the formation and presence of a network of SBs. In fact, during initial loading, the formation of SBs will contribute to the overall plastic deformation of the powders, whereas after full densification is achieved, the network of SBs enhances the overall plasticity of the BMG.

Deformation during HPT is highly localized in SBs, leaving most of the sample undeformed. The TEM images of the HPTed MgCuGd BMG, shown in Figure 2, were taken from positions corresponding to the center of the HPTed BMG, both in thickness and in radial directions. The TEM images reveal the presence of a featureless amorphous phase. Neither precipitates nor any type of phase contrast was evident in these amorphous regions of the sample. In addition to revealing the presence of a high density of SBs in the TEM images of the HPTed MgCuGd BMGs, the extended SBs were measured to have widths ranging from 50–400 nm, and an average of 214 nm; this is in contrast to published work which reports SB width values of 10–20 nm [14–16].

The physical characteristics of SBs provide insight into the deformation of MgCuGd BMG during HPT. In related work, it was reported that the formation of SBs results in local planar heating, which can cause local heating above T_g, crystallization as shown in Figure 2, and even possible melting. The temperature profile, ΔT, as a function of t and of distance x from the SBs can be determined from [7]:

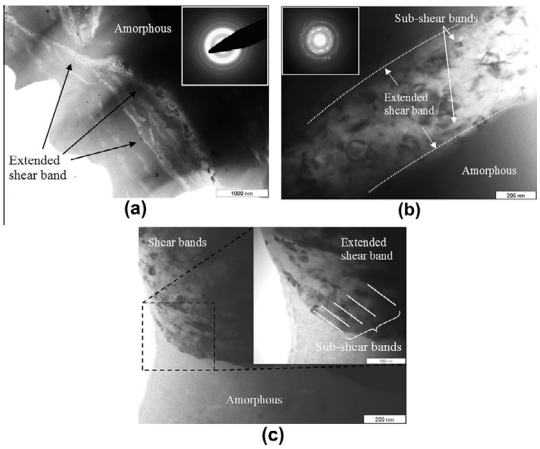

Figure 2. Extended SBs in HPTed MgCuGd BMG: (a) low-magnification TEM image with SAED pattern; (b) magnified TEM image of local SBs with SAED pattern; and (c) sub-SBs inside extended SBs.

$$\Delta T = \left(\frac{H}{2\rho C\sqrt{\pi\alpha}}\right)\frac{1}{\sqrt{t}}\exp\left(\frac{-x^2}{4\alpha t}\right), \quad (1)$$

where H is the heat content, ρ is the density of the material, C is the specific heat and α is the thermal diffusivity. Generally, the temperature increases by thousands of degrees during a very short time interval (from nanoseconds to seconds) [7]. The local heating at a SB results in a normal distribution in the temperature profile along the cross-section of a SB. When high local heating reaches T_g or T_x, viscosity inside the SBs suddenly decreases, resulting in superplastic deformation of the metallic glass localized into SBs. In conventional uniaxial tensile and compressive deformation, the initiation and propagation of SBs is generally instantaneous, leading to catastrophic brittle failure of BMGs; hence there is not sufficient time for the SB width to increase. In contrast, the presence of high hydrostatic pressure during HPT effectively suppresses crack nucleation and the continuous shear deformation in the SBs causes local heating, which promotes thickening of the SBs and localized crystallization of nc grains in the extended SBs.

It is worth noting that close inspection of the extended SBs reveals the presence of nc grains with an approximate size of 62 nm, as shown in Figure 2b. The nc grains are responsible for the rings in the SAED pattern shown in the inset figure. It has been reported that crystallization was observed inside or in the vicinity of SBs in BMGs [17,18]. The presence of nc grains within the SBs can be attributed to local planar heating generated during highly localized shear deformation [7]. Moreover, it was also observed that there were some sub-SBs in the vicinity of the interface formed between the crystallites and the amorphous matrix in the primary extended SBs. Figure 2c shows a high-magnification view of four sub-SBs located inside one SB, ~400 nm thick. The width of the sub-SBs ranges from 15 to 45 nm, and increases as one moves from the center to the edge of the SBs. Extended exposure to high localized heating in the vicinity of SBs during HPT results in the crystallization of high-density nc grains in the primary SBs. Consequently, shear deformation remains localized in these extended and crystallized SBs, and promotes the formation of sub-SBs, as illustrated in Figure 2c. It has been reported that shear banding is also the dominant mode of plastic deformation in body-centered cubic Fe [19], face-centered cubic Ni [20] and hexagonal close-packed Ti [21] metals when the grain sizes are nc. In these studies, the grains inside the sub-SBs are heavily elongated, with a large true strain of ~2. Slightly coarser grains with equiaxed geometry were observed in the center region of extended SBs, as compared to the grains in sub-SBs.

The density and width of SBs increase as a function of radial distance from the center of HPTed BMG, which is consistent with the associated increase in strain towards the edge of the disc. The nominal effective shear strain can be estimated on the basis of following equation: $\gamma = 2\pi RN/t$, equivalent to a true accumulated strain $\varepsilon = \ln(2\pi RN/t)$ [3], where N is the number of rotations, R is the distance from the center of the rotation and t is the thickness. The deformation shear strain increases from the center to the edge of an HPTed BMG; decreases with increasing sample thickness; and increases with increasing number of HPT turns. The density and width of SBs increase with increasing number of HPT turns.

Figure 3a shows DSC curves corresponding to as-atomized MgCuGd powders and HPTed BMGs, as determined using a heating rate of 20 K min^{-1}. The glass transition temperatures, T_g, reveal only a negligible increase, whereas the crystallization onset temperature, T_x decreases significantly after HPT. T_x decreases from 479 to 460 K for the HPTed MgCuGd BMG. It is likely that structural relaxation occurred in the HPTed BMGs as T_x decreased, which is a result of the strain energy introduced during HPT before crystallization eventually occurs [22]. The physical mechanism of structural relaxation in BMGs involves stress relief, atomic movement and the annihilation of excess free volume. Both high pressure and shear deformation during HPT can promote short-range atomic rearrangement in BMGs by reducing the free volume. We propose that in our experiments, SB formation was assisted by the extreme localization of shear in terms of a structural change, a

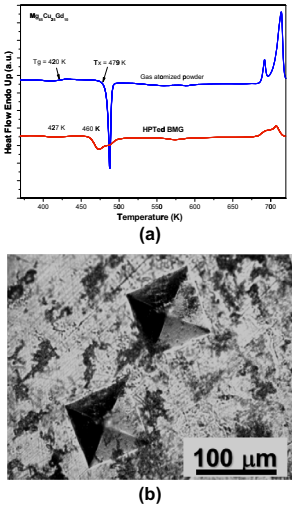

Figure 3. (a) DSC curves of HPTed MgCuGd BMG compared with starting MgCuGd powder; and (b) Vickers microhardness indentation with 1000 g load.

temperature rise and a local viscosity decrease in the bands. It is known that there are three stages for initial SB formation [17]: the multiplication of free volume; the coalescence of free volume and formation of voids; and the final fast propagation of SBs/cracks. Therefore, the formation of SBs is also closely related to local structural relaxation, which is consistent with our results. In the case of HPTed BMG, it is also interesting to note that two-step crystallization occurs, which may be attributed to precipitation of other intermetallic compounds from the amorphous phase in addition to the suggestion of structural relaxation; however, precise determination of the origin of this phenomena requires additional investigation.

Because of the sample size and geometry, only microindentation deformation studies with different applied loads, 50–1000 g, were carried out. The results show that indentation size increases linearly with applied load. An average Vickers microhardness value of ~306HV was obtained from measurements across the HPTed MgCuGd, which corresponds to an approximate strength of 1000 MPa from microhardness values [14], assuming strength ≈ hardness/3. It is interesting to note that no cracks were evident in the samples, even for large indents obtained with a 1000 g load force, as shown in Figure 3b. This apparent ductility may be rationalized based on the presence of existing multiple SBs, which contribute to shear softening, and therefore plasticity, during indentation. It is well known that crystalline metallic materials can exhibit high macroscopic plastic deformation due to multiple cross-slip. Similarly, our results suggest that it is possible to introduce large amounts of plasticity into BMGs by generating a high density of multiple and interacting SBs under high superimposed hydrostatic stress. The low shear modulus in SBs [6] allows for shear collapse before the extensional instability of crack formation can occur.

The presence of nc in the extended SBs may also have contributed to the overall plasticity of the MgCuGd BMGs by acting as "soft" inclusions relative to the hard matrix. In related studies it was reported that the introduction of "soft" inhomogeneities, such as dendrites, in a BMG matrix can assist in the nucleation of local SBs in the vicinity of these inhomogeneities [13].

Figure 4 provides a schematic diagram illustrating the influence of shear deformation during HPT on the resultant stress–strain response, and can be described as follows. In the case of a primarily tensile stress state, SBs nucleate and rapidly evolve into cracks without much growth, resulting in catastrophic brittle failure before yielding (Fig. 4a). In the case of a uniaxial compressive stress state (Fig. 4b), thin SBs nucleate in the BMG matrix, and continue to deform slightly beyond yielding due to compressive stress confining the SB. Finally, in the case of high superimposed hydrostatic compressive stress (Fig. 4c), such as HPT, multiple extended SBs nucleate in the BMG matrix and continue to deform and interact during deformation, possibly even leading to strain-softening [11].

In summary, Mg-based MgCuGd BMGs were successfully fabricated via HPT consolidation directly from gas-atomized powders. High-density extended SBs containing nc grains developed during HPT of MgCuGd

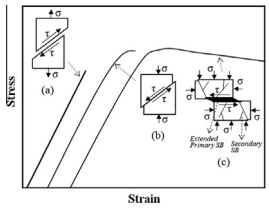

Figure 4. Schematic illustration of SB evolution in BMGs as a function of shear strain and stress states with: (a) tensile stress; (b) uniaxial compressive stress; and (c) hydrostatic compressive stress.

BMG, and this phenomenon was attributed to the combination of intense shear deformation under an imposed hydrostatic pressure.

The authors acknowledge the financial support provided by the US Army Research Office (W911NF-10-1-0512 and W911NF-13-1-0405).

[1] B. Zheng, Y. Lin, Y. Zhou, E.J. Lavernia, Metal. Mater. Trans. B 40B (2009) 768–778.
[2] A. Inoue, Prog. Mater. Sci. 43 (1998) 365–520.
[3] A.P. Zhilyaev, T.G. Langdon, Prog. Mater. Sci. 53 (2008) 893–979.
[4] R.Z. Valiev, R.K. Islamgaliev, I.V. Alexandrov, Prog. Mater. Sci. 45 (2000) 103–189.
[5] R. Pippan, S. Scheriau, A. Hohenwarter, M. Hafok, Mater. Sci. Forum 584–586 (2008) 16–21.
[6] X. Lei, Y. Wei, Z. Hu, W.H. Wang, Philos. Mag. Lett. 93 (2013) 221–230.
[7] J.J. Lewandowski, A.L. Greer, Nat. Mater. 5 (2006) 15–18.
[8] Y.H. Liu, G. Wang, R.J. Wang, D.Q. Zhao, M.X. Pan, W.H. Wang, Science 315 (2007) 1385–1388.
[9] M. Yan, P. Yu, K.B. Kim, J.K. Lee, G.B. Schaffer, M. Qian, Scr. Mater. 62 (2010) 266–269.
[10] B. Zheng, D. Ashford, Y. Zhou, S.N. Mathaudhu, J.-P. Delplanque, E.J. Lavernia, Acta Mater. 61 (2013) 4414–4428.
[11] S.N. Mathaudhu, J. Taek-Im, R.E. Barber, I.E. Anderson, I. Karaman, K.T. Hartwig, Mater. Res. Soc. Symp. Proc. 754 (2003) CC3.5.1–8.
[12] Y. Lin, E.J. Lavernia, Metall. Mater. Trans. A 37 (2006) 3317–3322.
[13] D.C. Hofmann, J.Y. Suh, A. Wiest, G. Duan, M.L. Lind, M.D. Demetriou, W.L. Johnson, Nature 451 (2008) 1085–1089.
[14] A.E. Giannakopoulost, P.L. Larsson, R. Vestergaard, Int. J. Solids Struct. 31 (1994) 2679–2708.
[15] C.Q. Chen, Y.T. Pei, O. Kuzmin, Z.F. Zhang, E. Ma, J.T.M.D. Hosson, Phys. Rev. B 83 (2011) 180201–180203.
[16] O.V. Kuzmin, Y.T. Pei, C.Q. Chen, J.T.M. De Hosson, Acta Mater. 60 (2012) 889–898.
[17] D.T.A. Matthews, V. Ocelík, P.M. Bronsveld, J.T.M. De Hosson, Acta Mater. 56 (2008) 1762–1773.
[18] K. Hajlaoui, A.R. Yavari, B. Doisneau, A. LeMoulec, W.J. Botta, F.G. Vaughan, A.L. Greer, A. Inoue, W. Zhang, Å. Kvick, Scr. Mater. 54 (2006) 1829–1834.
[19] A. Khalajhedayati, T.J. Rupert, Acta Mater. 65 (2014) 326–337.
[20] J. Xie, X. Wu, Y. Hong, Scr. Mater. 57 (2007) 5–8.
[21] J. Peirs, W. Tirry, B. Amin-Ahmadi, F. Coghe, P. Verleysen, L. Rabet, D. Schryvers, J. Degrieck, Mater. Charact. 75 (2013) 79–92.
[22] A. Castellero, B. Moser, D.I. Uhlenhaut, F.H.D. Torre, J.F. Löffler, Acta Mater. 56 (2008) 3777–3785.